View Article Online
View Journal

NJC

Accepted Manuscript

This article can be cited before page numbers have been issued, to do this please use: S. Pandey, D. Bansal and R. Gupta, *New J. Chem.*, 2018, DOI: 10.1039/C8NJ00734A.

ROYAL SOCIETY OF CHEMISTRY

rsc.li/njc

View Article Online
DOI: 10.1039/C8NJ00734A

Journal Name RSCPublishing

ARTICLE

A metalloligand appended with benzimidazole rings: Tetranuclear [$CoZn_3$] and [$CoCd_3$] complexes and their catalytic applications

Cite this: DOI: 10.1039/x0xx00000x

Saurabh Pandey,[a] Deepak Bansal[a] and Rajeev Gupta[a,*]

Received 00th January 2012,
Accepted 00th January 2012

DOI: 10.1039/x0xx00000x

www.rsc.org/

A novel Co^{3+}-based metalloligand **1** offering appended benzimidazole rings has been prepared and utilized for the synthesis of tetranuclear [$CoZn_3$] (**2** and **2-Cl**) and [$CoCd_3$] (**3**) heterometallic coordination complexes (HCCs). Crystallographic studies of **2-Cl** and **3** illustrate coordination of three secondary metal ions (Zn^{2+}/Cd^{2+}) to the appended benzimidazole rings of **1** thus producing tetranuclear HCCs. Both HCCs were utilized as the heterogeneous catalysts for Knoevenagel condensation and Henry reactions. The stability and recyclability experiments illustrate stable nature of both HCCs during the catalysis.

Introduction

Heterometallic coordination complexes (HCCs) including heterometallic coordination polymers (HCPs) have always attracted scientific community due to their intriguing architectures and the presence of at least two different metals in close proximity.[1-3] The persistent development in this field is due to their potential applications as/in molecular magnetism,[4] luminescence,[5] sensing,[6] optics,[7] redox-properties[8] and catalysis.[9] HCCs have been mostly developed using compartmental ligands offering selective binding groups for coordinating two different metal ions.[10] In such an approach, it is important to recognize both electronic and geometrical requirements of two different metals which make the synthesis of HCCs challenging and thus restricting their growth.[11] The alternate route is to utilize a metalloligand which already contains a primary metal ion whereas its appended functional groups could be employed to coordinate a secondary metal ion.[12-14] The metalloligand approach provides several advantages over the conventional use of compartmental ligands. The prominent ones are the ease of selection of secondary metal ions[15] and a precise control over the dimensionality of the resultant materials.[16] Therefore, extensive research has been devoted to develop assorted metalloligands for the synthesis of versatile HCCs.[17-20] However, a critical challenge is to stop at the HCCs level and not allow a metalloligand to go all the way to produce HCPs. In this context, our research group has developed a variety of metalloligands for the subsequent synthesis of both HCCs and HCPs.[21-25] Over the course of metalloligand design, we realized that both HCCs and HCPs with accessible metal sites are excellent candidates for various catalytic application.[24,25] It is well-established that for an efficient catalytic system; size, charge, and coordination environment of a catalytic metal are critical parameters in dictating the catalysis outcome.[24,25] On the other hand, both stability and robustness of a catalyst remain important criteria.[24,25] In this work, we report a new Co^{3+}-based benzimidazole-appended metalloligand with its unique ability to coordinate three secondary metals ion to afford tetranuclear HCCs. The resultant tetranuclear [$CoZn_3$] and [$CoCd_3$] HCCs have been utilized as the heterogeneous catalysts for Knoevenagel condensation and nitro-Aldol (Henry) reactions.

Results and Discussion

Synthesis and characterisation of metalloligand 1

Synthesis of metalloligand **1** involves reaction of ligand H_2L in its deprotonated form, L^{2-}, with Co(II) salt followed by aerial oxidation (Scheme 1).[23a,23b,25b] In FTIR spectrum, both absence of amidic –NH stretches and bathochromically shifted $\nu_{C=O}$ stretches confirm coordination via deprotonated $N_{amidate}$ groups (Figure S1, ESI).[23a,23b,25b] The stretches at ca. 3315 cm^{-1} correspond to –NH groups of the appended benzimidazole rings.[26] ^1H NMR spectrum of **1** shows a doublet and a triplet at 8.05 and 8.46 ppm corresponding to pyridyl protons whereas benzimidazole ring protons were observed between 6.77 – 7.14 ppm (Figure S2, ESI). The benzimidazole –NH protons were observed at 11.67 ppm. UV-vis spectrum of **1** in *N*,*N*-dimethylformamide (DMF) exhibits a broad band at ca. 680 nm corresponding to *d-d* transition (Figure S3, ESI).[23a,23b,25b,25c] Conductivity measurement confirms a 1:1 electrolytic nature of this complex.[27]

View Article Online
DOI: 10.1039/C8NJ00734A

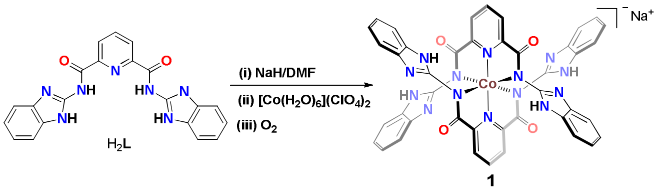

Scheme 1. Preparation route for the synthesis of metalloligand **1**.

Metalloligand **1** was crystallographically characterised and displays a Co(III) ion coordinated by four elongated $N_{amidate}$ and two compressed $N_{pyridine}$ bonds (Figure 1a). The Co(III) ion displays an octahedral environment in a bis-chelated ligand environment. Such a coordination mode has been observed in our earlier metalloligands appended with pyridyl, arylcarboxylate, thiazole and thiazoline groups.[22,25] In **1**, four $N_{amidate}$ groups constitute a basal plane while two $N_{pyridyl}$ atoms occupy the axial positions. The Co-$N_{amidate}$ bond distances were longer than that of Co-$N_{pyridyl}$ as observed earlier.[21–25] The unit cell of **1** displays the presence of two metalloligands connected together via two sodium ions (Figure 1b). Every Na^+ ion is coordinated to benzimidazole-N11 and amide-O4 atoms from one metalloligand and benzimidazole-N12 of a second one while the fifth coordination site is occupied by a methanol molecule. The involvement of benzimidazole-N coordination to Na^+ ions suggests the potential of metalloligand **1** in coordinating other secondary metal ions. Thus, reaction of **1** was performed with suitable secondary metal salts.

Heterometallic coordination complexes 2 and 3

Metalloligand **1** on reaction with acetate salts of Zn^{2+} and Cd^{2+} in MeOH produced tetranuclear HCCs [$CoZn_3$] (**2**) and [$CoCd_3$] (**3**), respectively (Scheme 2). FTIR spectra of **2** and **3** exhibited $\nu_{C=Oamide}$ stretches at ca. 1560 and 1546 cm^{-1}, respectively (Figure S4, ESI) that were blue-shifted (25–35 cm^{-1}) when compared to **1**. Super-imposable FTIR spectra of **2** and **3** suggest their isostructural nature. The diffused-reflectance absorption spectra of both HCCs exhibited λ_{max} at ca. 660 nm accompanied with a shoulder at ca. 500 nm (Figures S5 and S6, ESI). Notably, absorption spectra of **2** and **3** closely match to that of **1** thus suggesting that coordination of secondary metal ions has not dramatically influenced the electronic environment of the Co^{3+} ion. X-ray powder diffraction patterns of both HCCs **2** and **3** exhibited close match with the simulated patterns obtained from the single crystal diffraction data of **3** (Figures S7 and S8, ESI). Such a fact infers the structural similarities of both HCCs **2** and **3**, particularly in absence of the crystal structure of **2**. Both **2** and **3** were further investigated by thermogravimetric analysis (TGA) to understand the nature of coordinated and/or lattice solvent molecules (Figures S9, ESI). TGA for **2** and **3**, within the temperature range of 50 - 375 °C, exhibited weight changes of 19.28% (calc. 19.91%) and 25.85% (calc. 26.29%), respectively; corresponding to the loss of two DMSO, three acetate and two water molecules. A close similarity between the two samples further establishes a nearly identical structure and chemical composition of both HCCs.

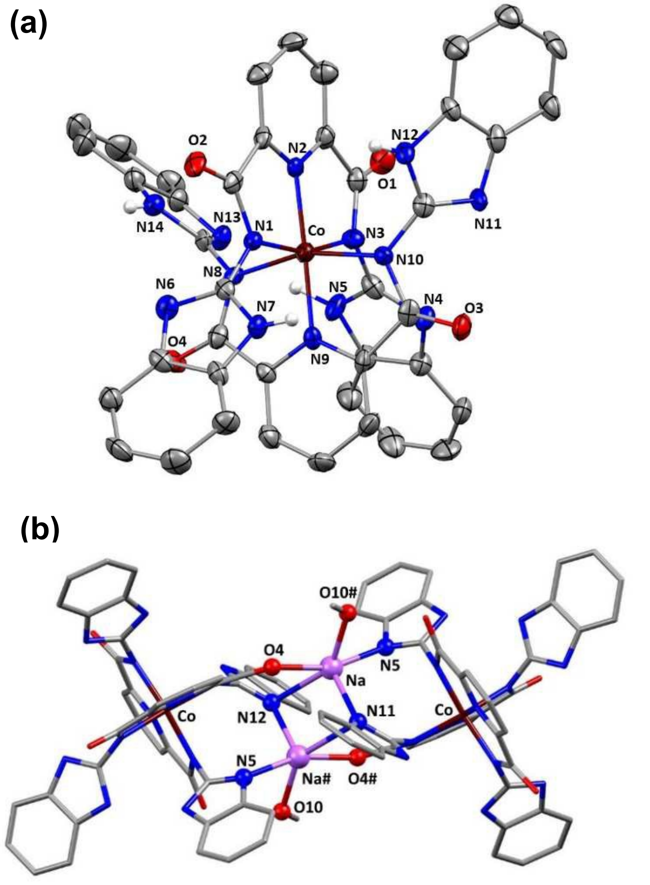

Figure 1. (a) Thermal ellipsoidal representation of complex **1** where ellipsoids are drawn at 50% probability level. Only selected hydrogen atoms are shown whereas sodium ion and lattice solvent molecules are omitted for clarity. (b) Capped and stick model showing dimeric structure of **1** after association involving Na^+ ions.

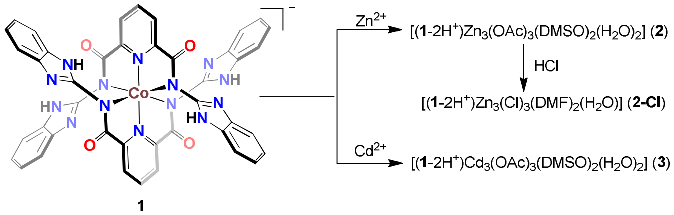

Scheme 2. Preparative route for the synthesis of heterometallic coordination complexes (HCCs) **2**, **2-Cl** and **3**.

Crystal structures of HCCs 2-Cl and 3

We next attempted to crystallize HCCs **2** and **3** to understand the coordination behaviour of metalloligand **1** towards secondary Zn^{2+} and Cd^{2+} ions. Importantly, while **3** was successfully crystallized from DMSO-EtOAc, single crystals of **2** suitable for X-ray diffraction could not be obtained. However, addition of a few drops of 2N HCl to a solution of **2** in DMF resulted in the crystallization of a new compound, **2-Cl**. Gratifyingly, crystal structures of both HCCs, [$CoZn_3$] (**2-Cl**) and [$CoCd_3$] (**3**), only differed by the type of anion and solvent molecules coordinated to the secondary metal ions. Notably, metalloligand **1** presents four benzimidazole rings to coordinate secondary metal ions. The crystal structures of both

HCCs (**2-Cl** and **3**) exhibited the involvement of all four appended benzimidazole rings in coordination to the secondary metal ions. As observed in the structure of **1**, both **2-Cl** and **3** displayed Co^{3+} ion in a N_6 coordination environment. Notably, Co^{3+}–N_6 core in HCCs **2-Cl** and **3** largely remained unaffected by the coordination of secondary metal ions as was observed with our earlier metalloligands (Table 1).[21,22]

Both HCCs, **2-Cl** and **3**, were isostructural except coordinated anions and solvent molecules. The crystal structure of **2-Cl** exhibits the presence of one metalloligand, three secondary Zn^{2+} ions, three coordinated chloride ions, one coordinated water and two coordinated DMF molecules. It is important to mention that the positive charge from three divalent Zn(II) ions is balanced by the presence of three chloride ions, one mono-anionic metalloligand and two deprotonated appended benzimidazole rings. Importantly, all appended benzimidazole rings are coordinated to three Zn^{2+} ions. For example, each Zn(II) ion is connected by two converging benzimidazole rings in addition to a chloride anion and a solvent molecule. The τ_4 values for three Zn(II) ions were 0.88 (Zn1), 0.90 (Zn2) and 0.93 (Zn3) thus suggesting a predominantly tetrahedral geometry.[28] The remaining two benzimidazole-N atoms (N6 and N14) remain uncoordinated and are present in protonated form.

The crystal structure of **3** reveals the presence of one metalloligand, three Cd^{2+} ions, three acetate ions, two coordinated DMSO and two coordinated H_2O molecules. The charge due to three Cd^{2+} ions is balanced by three acetate ions, a mono-anionic metalloligand and two deprotonated benzimidazole rings. Four appended benzimidazole rings provide eight nitrogen atoms, out of which six nitrogen atoms (N4, N5, N7, N11, N12 and N13) coordinate with three Cd(II) ion(s) whereas the remaining two uncoordinated benzimidazole rings are present in the protonated form as was also noted in **2-Cl**. The acetate ions coordinate to Cd^{2+} ions in a bidentate manner.[29] Among three cadmium ions, Cd1 and Cd3 exhibit five-coordinated distorted square-pyramidal geometry with two $N_{benzimidazole}$ and two $O_{acetate}$ atoms creating a basal plane and an axial DMSO molecule. The τ_5 values for Cd1 and Cd3 atoms were found to be 0.04 and 0.13, respectively therefore suggesting a predominantly square-pyramidal geometry.[30] The geometry around the third cadmium ion (Cd2) can be best described as the distorted octahedral where two $N_{benzimidazole}$ and two $O_{acetate}$ atoms comprise the basal plane whereas two water molecules are axially coordinated.

A closer investigation of both crystal structures revealed as to why only three and not four secondary metals are coordinated to metalloligand **1**. Interestingly, in both cases, coordination of three secondary metals resulted in a constrained geometrical alignment of the appended benzimidazole rings. As shown for HCC **3** in Figure 3, benzimidazole rings coordinated to a secondary metal exhibited N···N separation in the range of 3.660–3.682 Å. In contrast, uncoordinated benzimidazole rings display a much larger separation of their nitrogen atoms (N6…N14: 5.324 Å). Consequently, such an enhanced N···N separation did not result in enough convergence of two benzimidazole rings and as a result did not support coordination to a fourth secondary metal ion. Similarly, in **2-Cl**, Zn-coordinated benzimidazole rings show N···N separation of 3.407–3.469 Å whereas uncoordinated nitrogen atoms were separated by 5.779 Å (Figure S10, SI). Nevertheless, both HCCs present an unusual example of incorporating three secondary metal ions to a single metalloligand.

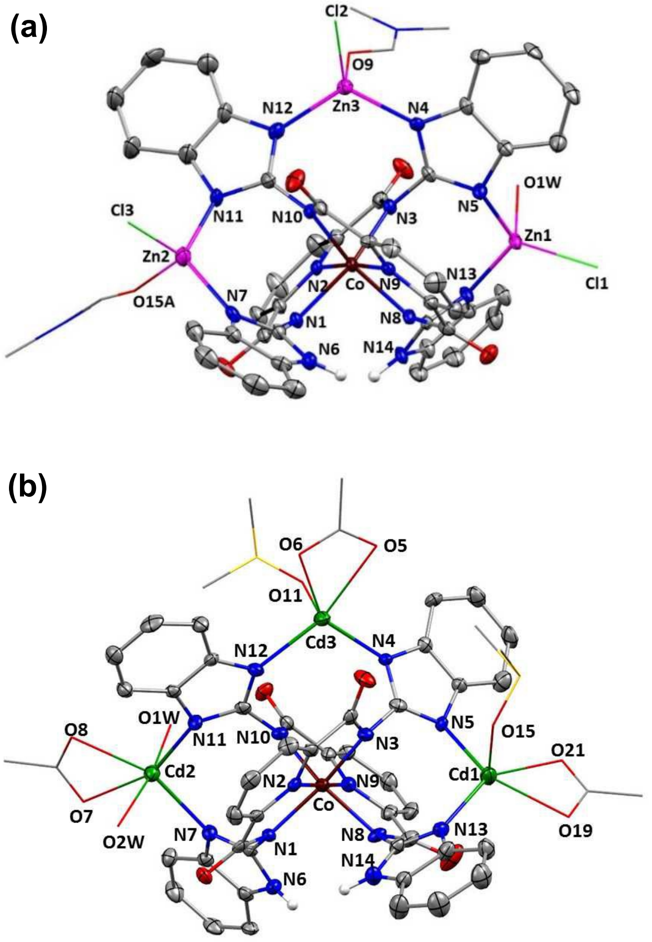

Figure 2. Thermal ellipsoidal representations of HCCs (a) **2-Cl** and (b) **3**. Thermal ellipsoids are drawn at 50% probability level whereas only selected hydrogen atoms are shown and lattice solvent molecules are omitted for clarity.

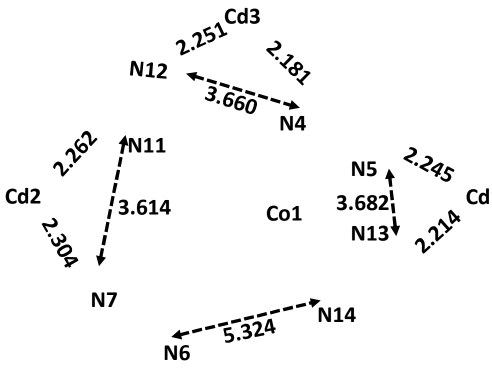

View Article Online
DOI: 10.1039/C8NJ00734A

Figure 3. A truncated structure of HCC **3** showing various bond distances between Cd(II) ions and separations between two neighbouring nitrogen atoms. The organic framework around the Cd(II) ions and coordinated solvents/ anions are removed for clarity.

Table 1. Selected bond distances (Å) and angles (˚) for complexes **1**, **2-Cl** and **3**.

Bond	1	2-Cl	3
Avg. Co-N_{amide}	1.953	1.953	1.960
Avg. Co-$N_{pyridyl}$	1.859	1.867	1.872
M(1)-N(5)	--	1.999(4)	2.244(5)
M(1)-N(13)	--	2.010(4)	2.213(5)
M(2)-N(7)	--	2.010(4)	2.377(4)
M(2)-N(11)	--	1.977(4)	2.262(5)
M(3)-N(4)	--	2.002(4)	2.181(5)
M(3)-N(12)	--	2.002(4)	2.252(5)

Where M = Zn^{2+} (for **2-Cl**) and Cd^{2+} (for **3**).

Heterogeneous catalysis

Lewis acidic metals have been subjected to detailed investigations due to their role in promoting numerous organic transformations.[31] Conventional Lewis acid catalysts are often based on main group as well as early transition metals;[31] however, late d-block metals such as zinc and cadmium have been particularly noteworthy.[9,32] Although various Zn- and Cd-based homogeneous catalysts have been developed but the quest for the recyclable and reusable heterogeneous catalysts has continued.[9,32] Crystal structures of both HCCs illustrate the presence of three exposed Lewis acidic metals (Zn^{2+} and Cd^{2+}) and weakly coordinated solvent molecules. These structural features prompted us to utilize both HCCs as the catalysts for the Lewis acid assisted catalytic reactions.[9] In Lewis acid catalyzed reactions, typically activation of a substrate is a prerequisite and plays a critical role before its transformation into a product.[21a,21b] The presence of weakly coordinated solvents to the Lewis acidic metals suggests that they could be easily removed and/or replaced to facilitate the access of a substrate.[2a,25b] In order to avoid competition from the solvent molecule(s), we planned to utilize both HCCs as the heterogeneous catalysts. To investigate potential catalytic applications of both HCCs, Knoevenagel condensation reactions (KCRs)[33,34] and Henry reactions (HRs)[33] were selected as both these reactions are known to be catalyzed by Lewis acidic metals.[25b–25d,34,35] Notably, both these reactions are good yet facile synthetic tools for the construction of C-C bonds.[34,35]

In a typical KCR, benzaldehyde reacted smoothly with malononitrile in presence of only 0.5 mol% of catalyst under the solvent-free conditions to give 2-benzylidene-malononitrile as the only product.[25b–25d] The completion of the reaction at room temperature (25±1 °C) that too within 75 min illustrates the noteworthy catalytic performance of both HCCs (Table 2). In order to confirm that HCCs indeed drive KCRs, catalytic reactions were also performed using metalloligand **1** as a catalyst. As expected, metalloligand **1** produced negligible product (<5%) for a reaction between benzaldehyde and malononitrile under the otherwise identical reaction conditions.

Both **2** and **3** further supported the reaction of malononitrile with different substituted aldehydes to afford the respective products. Interestingly, electronic and steric properties of the substituted aldehydes influenced the product yield to some extent.[25b,25c] For example, while electron-withdrawing substituents on benzaldehyde (entry 2) increased the product yield; electron-donating ones (entries 3 and 4) resulted in lower product formation. Moreover, reaction with bulkier substrates, such as 1-naphthaldehyde, 2-napthyldehyde and 9-anthraldehyde, resulted in reduced yield as compared to benzaldehyde (entries 5-7). Such a fact suggests that bulkier substrates have restricted access towards the catalytic secondary metal sites decorated on a metalloligand.[25b,25c] Importantly, as shown in Table 2, product yields were better for HCC **3** when compared to **2**. We tentatively propose that such an observation is primarily related to the better accessibility of a substrate to the catalytic Cd(II) ion due to its larger size.[25b,25c,36]

Table 2. Knoevenagel condensation reactions (KCRs) of assorted aldehydes with malononitrile using HCCs **2** and **3** as the catalysts.

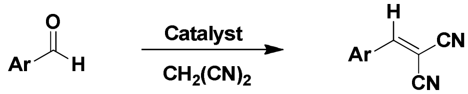

Entry[a]	Ar	% Yield[b]	
		2	3
1	C_6H_5	79, 77[c], 76[d]	>99, 98[c], 96[d]
2	*p*-$NO_2C_6H_5$	87	97
3	*p*-$OCH_3C_6H_5$	74	94
4	*p*-ClC_6H_5	82	88
5	1-Naphthyl	73	85
6	2-Naphthyl	70	80
7	9-Anthryl	65	72

[a]Conditions: 0.5 mol% catalyst; 75 min, 25±1 °C. [b]Yield was determined by GC. [c]Isolated yield for the second run with reused catalyst. [d]Isolated yield for the third run with reused catalyst.

Motivated with successful KCRs, we next targeted nitro–aldol Henry reactions (HRs). HR is a simple C-C bond forming reaction between aldehydes or ketones with niroalkanes[35] It is important to note that there are limited reports on solvent-free HRs.[37] Majority of the reports require presence of a protic solvent such as MeOH or EtOH. This suggests possible involvement of a protic solvent during the reaction.[38] However, with the intention to exclude any solvent participation and potential advantage of heterogeneous catalysis; all reactions were performed in absence of any solvent. Interestingly, best conversion was obtained when 4-nitrobenzaldehyde was treated with nitromethane in presence of only 1 mol% of HCC **3** that afforded the respective β-nitroalkanol in 92 % yield (entry 3, Table 3). Therefore, optimization experiments were performed by the reaction of 4-nitrobenzaldehyde with nitromethane varying catalyst, temperature, solvent and time (Table 3). The catalytic results substantiate the importance of HCCs in HRs as no product was formed when metalloligand **1** was used as a catalyst. Similarly, no product formation was noticed with either nitrate or chloride salts of Zn^{2+} or Cd^{2+} as the catalysts (entries 5–8). However, utilization of

View Article Online
DOI: 10.1039/C8NJ00734A

$Zn(OAc)_2$ or $Cd(OAc)_2$ as the catalysts resulted in 8-10 % product formation (entries 9 and 10). Solvent screening experiments exhibited inferior catalytic results when compared to that of solvent-free reactions although use of MeOH still produced the product in 90% yield while other solvents were mostly moderately effective (entries 11 - 14). These finding suggest that the presence of a protic solvent indeed plays an important role in HRs[38] whereas solvent-free conditions mimic the significant role played by a protic solvent. We propose that the Lewis acidic metals in **2** and **3** better activate both substrate and nitromethane in absence of a solvent (vide infra) and help in driving the reactions.

Table 3. Control and optimization experiments for Henry reactions.

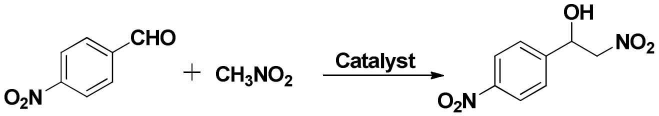

Entry[a]	Catalyst	Solvent	% Yield[b]
1	**1**	---	0
2	**2**	---	74
3	**3**	---	92
4	**2-Cl**	---	68
5	$ZnCl_2.2H_2O$	---	0
6	$CdCl_2.2H_2O$	---	0
7	$Zn(NO_3)_2.6H_2O$	---	0
8	$Cd(NO_3)_2.6H_2O$	---	0
9	$Zn(OAc)_2.2H_2O$	---	8
10	$Cd(OAc)_2.2H_2O$	---	10
11	**3**	CH_3OH	90
12	**3**	*tert* - BuOH	70
13	**3**	H_2O	42
14	**3**	CH_3CN	30

[a]Conditions: 1.0 mol% catalyst; 36 h, 60 °C. [b] Isolated yield.

After optimization of reaction conditions, we investigated the influence of electronic substituents on an aldehyde on the product yield (Table 4). For example, benzaldehydes substituted with electron-withdrawing nitro group (entries 2-4) exhibited better product yield as compared to benzaldehyde (entry 1). However, product yield was reduced when benzaldehyde was substituted with electron-donating groups (entries 5 and 6). Finally, use of sterically bulkier naphthaldehyde considerably reduced the product yield (entry 7). Such an observation supports KCRs where product yield depended on the steric bulkiness of a substrate that has most probably restricted the approach of a substrate towards the Lewis acidic secondary metals.

Table 4. Henry reactions of various aldehydes with nitromethane using HCCs **2** and **3** as the catalysts.

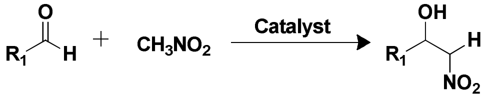

		% Yield	
Entry[a]	R_1	2[b]	3[b]
1	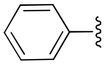	47	51
2	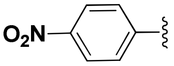	86	92
3	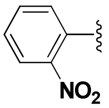	78	87
4	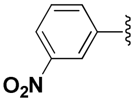	70	79
5	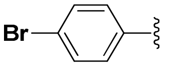	40	48
6	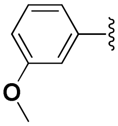	56	61
7	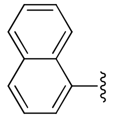	45	47

Conditions: 1.0 mol% catalyst; 36 h, 60°C. [b] Isolated yield.

As mentioned earlier, activation of a substrate is an important step during the catalysis. We believe that in both KCRs and HRs, activation of an aldehydic substrate takes place prior to the nucleophilic attack.[25b,25c] To prove such a postulate, both HCCs **2** and **3** were suspended in CH_2Cl_2 containing benzaldehyde. Such impregnated samples exhibited bathochromically shifted C=O stretches at 1693 (**2**) and 1694 (**3**) cm^{-1}, respectively (Figures S11 and S12, ESI) and were shifted by ca. 15 cm^{-1} when compared to neat C_6H_5CHO (1708 cm^{-1}).[23c] Such an observation suggests potential coordination of benzaldehyde and therefore its activation.[25b–25d] We also tested activation of nitromethane used in HRs with both HCCs. Similar impregnation experiments performed using nitromethane exhibited the appearance of $\nu_{N=O}$ band at 1540 cm^{-1} in **2** and 1524 cm^{-1} in **3** (Figures S13 and S14, ESI). Such $\nu_{N=O}$ bands were also red-shifted when compared to only nitromethane (1555 cm^{-1}).[39] Both these experiments suggest that benzaldehyde as well as nitromethane have potentially coordinated the secondary metals after replacing the loosely bound solvents and/or anion.

Reusability and recyclability experiments

To establish the true nature of heterogeneous catalysis, reactions between benzaldehyde and malononitrile was monitored using HCC **3** as a model catalyst. As can be seen from Figure 4, product formation ceased on removal of the catalyst **3** (red spheres) and resumes after its addition. This

View Article Online
DOI: 10.1039/C8NJ00734A

simple filtration experiment suggests that HCC **3** acts as a heterogeneous catalyst and other catalytically active species have not been leached out.[25] A simple filtration allowed easy recovery of both HCCs from the reaction mixture and their consecutive use for five cycles for a reaction between benzaldehyde and malononitrile (inset, Figure 4). During these cycles, both HCCs retained their catalytic ability without considerable decrease in the product yield. It is noteworthy to mention that no activation or purification was performed before reusing both HCCs.

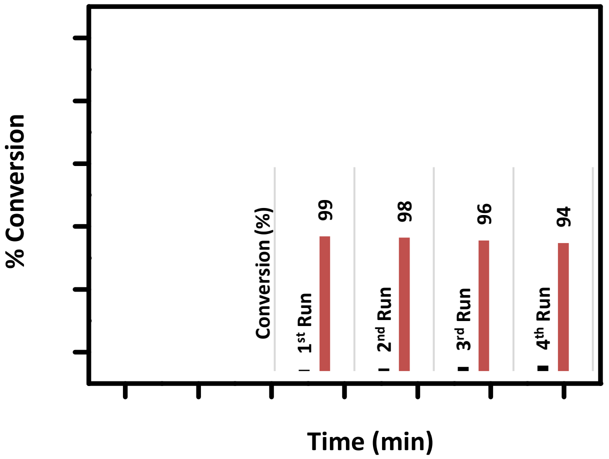

Figure 4. Filtration test during KCR between benzaldehyde and malononitrile in presence of HCC **3** as a catalyst displays that removal of **3** after 30 min lead to the cessation of catalysis whereas re-addition after ca. 60 min results in the resumption of the catalytic reaction. The inset displays recyclability of HCC **3** for four consecutive cycles.

In order to prove structural integrity and crystallinity of both HCCs during the Henry reaction of benzaldehyde with nitromethane; FTIR, XRPD and SEM studies were performed. FTIR spectra of recovered HCCs **2** and **3** after the catalysis nicely overlapped to that of pristine sample thus attesting to their stability during the catalysis (Figures S15 and S16, ESI). Similarly, XRPD patterns both for **2** and **3** exhibited a close match to that of as-synthesized sample suggesting that their crystallinity is maintained during the catalysis (Figures S17 and S18, ESI). Although SEM images of HCC **3** do suggest moderate decrease in crystal size after the catalysis; bulk material illustrated enough crystallinity required for the desirable recyclability (Figure 5). Collectively, these results confirm robust and stable nature of both HCCs **2** and **3** during the catalysis.

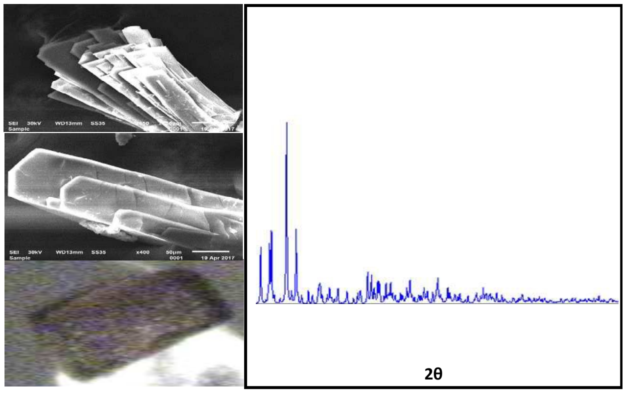

Figure 5. SEM micrographs (left panels) and XRPD patterns (right panels) of HCC **3**; (bottom) as synthesised, (middle) before catalysis and (top) after catalysis for the reaction between benzaldehyde and malononitrile.

Experimental Section

General

All reagents were purchased from the commercial sources and used without further purification. The solvents were dried and purified using standard procedures.[40] The ligand H_2L was synthesized as per our earlier report.[26a]

Na[Co(L$_2$)CH$_3$OH]·2CH$_3$OH (1). Ligand H_2L (0.5 g, 1.258 mmol) was dissolved in dinitrogen-flushed DMF (20 mL) and to it was added solid NaH (0.060 g, 2.516 mmol), resulting in a pale yellow solution. To the aforementioned mixture, solid $[Co(H_2O)_6](ClO_4)_2$ (0.230 g, 0.629 mmol) was added under dinitrogen atmosphere. The resulting solution was stirred for 2 h in open air during which colour changed to brownish-green. Removal of the solvent was followed by the addition of 25 mL of MeOH and filtration. Diethyl ether vapours were diffused through the methanol filtrate that afforded crystalline compound. The solid was collected by filtration and dried under vacuum. Yield: 0.8 g (66 %). $C_{45}H_{38}CoN_{14}NaO_7$ (968.79): calcd. C 55.79; H 3.95; N 20.24; found: C 56.05; H 4.12; N 19.77. FTIR spectrum (Zn–Se ATR, cm^{-1}): 3309 (N-H), 1624 (C=O) and 1522 (C=N) ^{1}H NMR spectrum (400 MHz, DMSO-d$_6$): δ = 11.86 (s, 2H), 8.46 (t, *J* = 7.4 Hz, 1H), 8.05 (d, *J* = 7.5 Hz, 2H), 7.14 (s, 2H), 6.80 (d, *J* = 21.1 Hz, 6H). ^{13}C NMR spectrum (100 MHz, DMSO-d$_6$): δ = 170.75 (s), 157.83 (s), 152.46 (s), 141.71 (s), 140.18 (s), 132.81 (s), 124.57 (s), 120.58 (s), 120.40 (s), 117.27 (s), 110.49 (s). Diffuse reflectance UV/Vis spectrum; 645 nm. UV/Vis spectrum (DMF): nm (ε M^{-1} cm^{-1}), 680 (175).

[(1)Zn$_3$(OAc)$_3$(H$_2$O)$_2$(DMSO)$_2$] (2). Complex **2** was synthesized by treating a solution of complex **1** (0.1 g, 0.103 mmol) in methanol (10 ml) with $Zn(OAc)_2$ (0.067 g, 0.309 mmol). The reaction mixture was stirred at room temperature for 2 h. The solid thus obtained was filtered and dried under vacuum. Yield 112 mg (77 %). $C_{52}H_{49}Zn_3CoN_{14}O_{14}.S_2$ (1413.23): calcd. C, 44.19; H, 3.49; N, 13.88; found C, 43.92; H, 3.58; N, 14.06. FTIR spectrum (Zn–Se ATR, cm^{-1}): 3184 (N-H), 1631 (C=O) and 1560 (C=N). Diffuse reflectance UV/Vis spectrum: λ_{max} 660 nm.

View Article Online
DOI: 10.1039/C8NJ00734A

$[(1)Zn_3(Cl)_3(H_2O)(DMF)_2]\cdot 3DMF$ (2-Cl). Complex **2** (100 mg) was dissolved in DMF (10 ml) followed by the addition of a few drops of 2N HCl solution. The resulting solution was diffused by the vapours of diethyl ether at room temperature. After one week, red colored crystalline material was obtained**.** The solid thus obtained was filtered and dried under vacuum. Yield: 72 mg (66.3 %). $C_{48}H_{40}Cl_3Zn_3CoN_{16}O_7\cdot 3C_3H_7NO$ (1533.65): calcd. C, 45.67; H, 5.26; N, 17.75; found C, 45.82; H, 4.88; N, 18.12. FTIR spectrum (Zn–Se ATR, cm^{-1}): 3190 (N-H), 1638 (C=O) and 1530 (C=N). Diffuse reflectance UV/Vis spectrum: λ_{max} 655 nm.

$[\{1(Cd)_3(OAc)_3(DMSO)_2(H_2O)_2\}]$ (3). To a solution of **1** (0.100 g, 0.103 mmol) in methanol was added a solution of $Cd(OAc)_2.2H_2O$ (0.067 g, 0.309 mmol) in MeOH (5 ml). A red colored compound was precipitated that was filtered, washed with methanol and dried under vacuum. Yield: 130 mg (81 %). $C_{52}H_{49}Cd_3CoN_{14}O_{14}S_2$ (1554.33): calcd. C, 40.18; H, 3.18; N, 12.62; found: C, 39.73; H, 3.40; N, 13.01. FTIR spectrum (Zn–Se ATR, cm^{-1}): 3217 (N-H), 1622 (C=O) and 1546 (C=N). Diffuse reflectance UV/Vis spectrum: λ_{max} 658 nm.

Physical measurements. Conductivity measurements were carried out in organic solvents with a digital conductivity bridge from Popular Traders, India (model number: PT 825). Elemental analysis data were obtained with an Elementar Analysen Systeme GmbH Vario EL-III instrument. The NMR spectroscopic measurements were carried out with a Jeol 400 MHz instrument. The FTIR spectra were recorded with a Perkin–Elmer FTIR 2000 or spectrum–two spectrometer. The absorption spectra were recorded with a Perkin–Elmer Lambda 25 spectrophotometer. X-ray powder diffraction (XRPD) studies were performed either with an X'Pert Pro from Panalytical or a Bruker AXS D8 Discover instrument (Cu-Kα radiation, λ = 1.54184 Å). The samples were ground and subjected to the range of θ = 2 –50° with a scan rate of 1° per minute at room temperature. Thermogravimetric analysis (TGA) was performed using a DTG 60 Shimadzu at 5 °C min^{-1} heating rate under the nitrogen atmosphere.

Crystallography. The intensity data for complexes **1** and **3** were collected on an Oxford XCalibur CCD[41] whereas for complex **2-Cl** on a Bruker SMART APEX CCD[42] respectively**,** by using graphite-monochromated Mo-*Kα* radiation (λ = 0.71073 Å). Intensity data were corrected for Lorentz polarization effects and an empirical absorption correction (SADABS) was applied.[43,44] The structures were solved by direct methods and refined by full-matrix least-squares refinement techniques on F^2 by using SHELXL-2016[45] in the WinGX module.[46] All hydrogen atoms were fixed at the calculated positions with isotropic thermal parameters whereas all non-hydrogen atoms were refined anisotropically. For complex **2-Cl**, one of the coordinated DMF molecule (O15, C100, N100, C101, C102) was found disordered and was refined isotropically. Moreover, oxygen atom O15 was fixed at two positions using part command. In addition, one of the –CH hydrogen atoms of the disordered DMF molecule could not be assigned however, is included in the molecular formula resulting in difference in the calculated and reported number of hydrogen atoms in the formulae. Furthermore, some disordered electron density could not be resolved and was therefore masked using the solvent masking 'Squeeze' command in PLATON.[47] The recovered electron count of 274 corresponded to nearly seven DMF molecules. In complex **3**, one coordinated and one lattice DMSO molecules were disordered and were fixed at two positions using part command. Moreover, all four carbon atoms (C49, C50, C53 and C54) of both these DMSO molecules were refined isotropically. Details of the crystallographic data collection and structure solution parameters are given in table 5. CCDC-1823596-1823598 contain the supplementary crystallographic data for this paper. These data can be obtained free of charge from The Cambridge Data Center via www.ccdc.cam.ac.uk/data_request/cif.

Table 5. Crystallographic data collection and structure refinement parameters for complexes **1**, **2-Cl** and **3**.

Complex	**1**	**2-Cl**	**3**
Formula	$C_{90}H_{70}Co_2N_{28}Na_2O_{14}$	$C_{111}H_{115}Cl_6Co_2N_{37}O_{19}Zn_6$	$C_{60}H_{73}Cd_3CoN_{14}O_{18}S_6$
Formula Wt.	1931.58	2994.17	1866.81
T (K)	293(2)	273(2)	253(2)
System	Monoclinic	Triclinic	Triclinic
Space group	*P*2*₁*/c	*P*-1	*P*-1
a (Å)	14.7170(8)	15.1412(13)	13.876(5)
b (Å)	16.7634(11)	17.3711(15)	14.859(5)
c (Å)	20.2352(11)	25.697(2)	20.392(5)
α (°)	90	79.384(2)	74.361(5)
β (°)	119.615(4)	84.626(3)	71.679(5)
γ (°)	90	86.773(3)	68.406(5)
V ($Å^3$)	4340.0(5)	6608.8(10)	3654(2)
Z	2	2	2
$\rho_{calc}(mg/m^3)$	1.478	1.503	1.697
μ (mm^{-1})	0.476	1.511	1.332
F (000)	1988	3048	1884
Goodness-of-fit (GOF) on F^2	0.987	1.027	1.026
Final R indices [$I > 2\sigma(I)$]	R_1 = 0.0705, wR_2 = 0.0877	R_1 = 0.0670, wR_2 = 0.1561	R_1 = 0.0675, wR_2 = 0.1162
R indices (all data)	R_1 = 0.1430, wR_2 = 0.1097	R_1 = 0.1247, $wR2$ = 0.1835	R_1 = 0.1213, wR_2 = 0.1375
CCDC No.	1823596	1823598	1823597

General procedure for the catalytic reactions. In a typical KCR, 1 equiv. of aldehyde was treated with malononitrile (2.5 equiv.) in presence of 0.5 mol% catalyst. In HR, aldehyde (1 equiv.) was reacted with either nitromethane or nitroethane (5 equiv.) in presence of 1.0 mol % catalysts. Both catalytic reactions were performed under solvent-free condition. For both KCR and HR, the reaction mixture was stirred for 75 min and 36 h, respectively. Reactions were monitored by using thin layered chromatography (TLC) and/or gas chromatography (GC). After mentioned time, the reaction was quenched by the addition of ethyl acetate and the catalyst was filtered off. The filtrate was concentrated under the reduced pressure. The crude compound was purified by using flash column chromatography on silica gel using hexanes–ethyl acetate mixture (5:1) as the eluent. The resultant product(s) was analyzed by GC and NMR spectral techniques. Representative ^{1}H NMR spectra of some of the isolated organic products are displayed in Figures S19 – S25, ESI.

View Article Online
DOI: 10.1039/C8NJ00734A

Characterization data of few representative products:

2-nitro-1-phenylethanol. Yield: 80 mg (51%). ^{1}H NMR spectrum (500 MHz, CDCl$_3$): δ 7.40 – 7.33 (m, 5H), 5.44 (d, J = 9.6 Hz, 1H), 4.59 (dd, J = 13.3, 9.7 Hz, 1H), 4.49 (dd, J = 13.3, 3.1 Hz, 1H), 3.03 (s, 1H).

2-nitro-1-(4-nitrophenyl)ethanol. Yield: 129 mg (92%). ^{1}H NMR spectrum (400 MHz, CDCl$_3$) δ 8.25 (d, J = 8.6 Hz, 2H), 7.62 (d, J = 8.8 Hz, 2H), 5.60 (dd, J = 8.1, 4.0 Hz, 1H), 4.59 (dd, J = 10.1, 3.6 Hz, 2H), 3.29 (s, 1H).

2-nitro-1-(4-nitrophenyl)propan-1-ol. Yield: 118 mg (79%). ^{1}H NMR spectrum (400 MHz, CDCl$_3$) δ 8.31 – 8.17 (m, 4H), 7.58 (dd, J = 8.4, 5.6 Hz, 4H), 5.55 (d, J = 2.6 Hz, 1H), 5.18 (d, J = 8.4 Hz, 1H), 4.84 – 4.63 (m, 2H), 3.05 (d, J = 19.2 Hz, 2H), 1.48 (d, J = 6.8 Hz, 3H), 1.38 (d, J = 6.9 Hz, 3H).

2-nitro-1-(2-nitrophenyl)ethanol. Yield: 122 mg (87%). ^{1}H NMR spectrum (500 MHz, CDCl$_3$) δ 8.08 (dd, J = 8.3, 1.1 Hz, 1H), 7.95 (dd, J = 8.0, 0.7 Hz, 1H), 7.74 (td, J = 7.6, 0.9 Hz, 1H), 7.57 – 7.53 (m, 1H), 6.05 (dd, J = 9.1, 1.9 Hz, 1H), 4.87 (dd, J = 13.9, 2.4 Hz, 1H), 4.55 (dd, J = 13.8, 9.1 Hz, 1H), 3.22 (s, 1H).

2-nitro-1-(3-nitrophenyl)ethanol. Yield: 111 mg (79%). ^{1}H NMR spectrum (500 MHz, CDCl$_3$) δ 8.31 (d, J = 1.5 Hz, 1H), 8.23 – 8.19 (m, 1H), 7.76 (d, J = 8.0 Hz, 1H), 7.60 (t, J = 8.0 Hz, 1H), 5.60 (dd, J = 8.7, 3.6 Hz, 1H), 4.63 – 4.57 (m, 2H), 3.34 (dd, J = 224.8, 135.2 Hz, 1H).

1-(4-bromophenyl)-2-nitroethanol. Yield: 63 mg (48%). ^{1}H NMR spectrum (400 MHz, CDCl$_3$) δ 7.53 (d, J = 8.4 Hz, 2H), 7.28 (d, J = 8.5 Hz, 2H), 5.43 (dd, J = 9.3, 2.8 Hz, 1H), 4.59 – 4.45 (m, 2H), 3.01 (s, 1H).

1-(3-methoxyphenyl)-2-nitroethanol. Yield: 88 mg (61%). ^{1}H NMR spectrum (400 MHz, CDCl$_3$) δ 7.95 (s, 1H), 7.27 (dd, J = 13.2, 6.4 Hz, 1H), 6.95 (d, 1H), 6.86 (dd, J = 8.7, 2.1 Hz, 1H), 5.44–5.40 (m, J = 9.5 Hz, 1H), 4.61 – 4.46 (m, 2H), 3.80 (s, 3H), 3.66 (s, 1H).

1-(naphthalene-1-yl)-2-nitroethanol. Yield: 65 mg (47%). ^{1}H NMR spectrum (400 MHz, CDCl$_3$) δ 8.12 (d, J = 8.5 Hz, 1H), 7.92 (d, J = 8.0 Hz, 1H), 7.86 (d, J = 8.2 Hz, 1H), 7.66 (t, J = 7.7 Hz, 1H), 7.57 (t, J = 7.4 Hz, 1H), 7.46 (t, J = 7.8 Hz, 1H), 7.33 (d, J = 7.1 Hz, 1H), 5.38 – 5.16 (m, 1H), 4.93 (s, 2H), 4.93 (d, J = 1.7 Hz, 1H).

Conclusions

This work illustrated the synthesis and characterization of a unique metalloligand **1** offering four appended benzimidazole rings. Metalloligand **1** was utilized for the synthesis of tetranuclear [Zn$_3$Co] (**2** and **2-Cl**) and [Cd$_3$Co] (**3**) heterometallic coordination complexes (HCCs). The crystallographic studies of **2-Cl** and **3** exhibited unusual coordination of three secondary Zn^{2+}/Cd^{2+} ions to the appended benzimidazole rings being offered by **1** thus producing tetranuclear HCCs. Both HCCs were utilized as the heterogeneous catalysts for Knoevenagel condensation and Henry reactions. The stability and recyclability experiments asserted stable nature of HCCs in catalysis. These HCCs not only demonstrated the importance of metalloligands in material design but also in developing stable functional materials.

Acknowledgements

RG acknowledges Science and Engineering Research Board, New Delhi (EMR/2016/000888) and the University of Delhi for the financial support. SP and DB respectively thank CSIR, New Delhi and UGC, New Delhi for their fellowships. Authors thank CIF-USIC at this university for the instrumental facilities including crystallographic data collection.

Notes and references

[a] Department of Chemistry, University of Delhi, Delhi-110007. E-mail: rgupta@chemistry.du.ac.in; Web: http://people.du.ac.in/~rgupta/; Fax: +91-11-2766-6605; Tel: +91-11-2766-6646 Ext. 172.

Electronic Supplementary Information (ESI) available: Figures for FTIR, ^{1}H and ^{13}C NMR, and UV-Vis spectra; TGA plots; powder XRD patterns; and tables for detailed bonding parameters. CCDC Nos: 1823596-1823598. See DOI: 10.1039/b000000x/

1 (a) T. R. Cook and P. J. Stang, *Chem. Rev*., 2015, **115**, 7001–7045; (b) R. Chakrabarty, P. S. Mukherjee and P. J. Stang, *Chem. Rev*., 2011, **111**, 6810–6918; (c) D. Maspoch, D. R. Molina, J. Veciana, *Chem. Soc. Rev*., 2007, **36**, 770–818.

2 (a) S. Srivastava, M. S. Dagur, A. Ali and R. Gupta, *Dalton Trans*., 2015, **44**, 17453–17461; (b) X.-Z. Li, P. -P. Hao, D. Wang, W. -Q. Zhang and L. -N. Zhu, *CrystEngComm*., 2012, **14**, 366–369.

3 (a) R. M. Haas, Z. Hern, S. Sproules and C. R. Hess, *Inorg. Chem*., 2017, **56**, 14738−14742; (b) A. Mishra, A. Ali, S. Upreti, M. S. Whittingham and R. Gupta, *Inorg. Chem*., 2009, **48**, 5234–5243; (c) M. U. Anwar, L. N. Dawe, S. S. Tandon, S. D. Bungec and L. K. Thompson, *Dalton Trans*., 2013, **42**, 7781–7794.

4 (a) P. Mahapatra, S. Ghosh, N. Koizumi, T. Kanetomo, T. Ishida, M. G. B. Drewd and A. Ghosh, *Dalton Trans*., 2017, **46**, 12095–12105; (b) K. Liua, W. Shia and P. Chenga, *Coord. Chem. Rev*., 2015, **289–290**, 74–122; (c) K. C. Mondal, A. Sundt, Y. Lan, G. E. Kostakis, O. Waldmann, L. Ungur, L. F. Chibotaru, C. E. Anson and A. K. Powell, *Angew. Chem., Int. Ed*., 2012, **51**, 7550–7554; (d) V. Chandrasekhar, P. Bag, W. Kroener, K. Gieb and P. Müller, *Inorg. Chem*., 2013, **52**, 13078–13086; (e) F. Pointillart, K. Bernot, R. Sessoli and D. Gatteschi, *Chem. – Eur. J*., 2007, **13**, 1602–1609; (f) I. A. Kühne, N. Magnani, V. Mereacre, W. Wernsdorfer, C. E. Ansona and A. K. Powell, *Chem. Commun*., 2014, **50**, 1882–1885.

5 (a) W. Bi, T. Wei, X. Lu , Y. Hui, J. Song, S. Zhao, W.-K. Wong and R. A. Jones, *New J. Chem*., 2009, **33**, 2326–2334; (b) E. J. Fernandez, A. Laguna, J. M. Lopez-de-Luzuriaga, M. Monge, M. Montiel, M. E. Olmosa and M. R. –Castillo, *Dalton Trans*., 2009, 7509–7518; (c) X. Zhang, B. Li, Z.-H. Chen and Z. –N. Chen, *J. Mater. Chem*., 2012, **22**, 11427–11441; (d) A. M. Nonat, C. Allain, S. Faulkner, and T. Gunnlaugsson, *Inorg. Chem*., 2010, **49**, 8449–8456

6 (a) X. Zhou, S. Lee, Z. Xu and J. Yoon, *Chem. Rev*., 2015, **115**, 7944−8000; (b) T. Wagner, S. Haffer, C.; Klaus, D. Weinberger and M. Tiemann, *Chem. Soc. Rev*., 2013, **42**, 4036–4053; (c) S. Srivastava, B. K. Gupta and R. Gupta, *Cryst. Growth Des*., 2017, **17**, 3907−3916.

7 (a) Z. Hu, B. J. Deibert and J. Li, *Chem. Soc. Rev*., 2014, **43**, 5815−5840; (b) V. Stavila, A. A. Talin and M. D. Allendorf, *Chem. Soc. Rev*., 2014, **43**, 5994−6010; (c) C. Wang, T. Zhang and W. Lin,

View Article Online
DOI: 10.1039/C8NJ00734A

Chem. Rev., 2012, **112**, 1084−1104; (d) M. D. Allendorf, C. A. Bauer, R. K. Bhakta and R. J. T. Houka, *Chem. Soc. Rev.*, 2009, **38**, 1330−1352; (e) J. -C. G. Bunzli and C. Piguet, *Chem. Rev.*, 2002, **102**, 1897−1928.

8 (a) K. Bhattacharya, S. M. T. Abtab, M. C. Majee, A. Endo and M. Chaudhury, *Inorg. Chem.*, 2014, **53**, 8287–8297; (b) X. Wu, T, Huang, T. T. Lekich, R. D. Sommer and W. W. Weare, *Inorg. Chem.*, 2015, **54**, 5322–5328.

9 (a) L. Q. Ma, C. Abney and W. B. Lin, *Chem. Soc. Rev.*, 2009, **38**, 1248–1256; (b) J. Liu, L. Chen, H. Cui, J. Zhang, L. Zhang and C.-Y. Su, *Chem. Soc. Rev.*, 2014, **43**, 6011–6061; (c) A. Dhakshinamoorthy and H. Garcia, *Chem. Soc. Rev.*, 2014, **43**, 5750–5765; (d) A. Corma, H. Garcia and F. X. L. I. Xamena, *Chem. Rev.*, 2010, **110**, 4606–4655; (e) J. Y. Lee, O. K. Farha, J. Roberts, K. A. Scheidt, S. B. T. Nguyen and J. T. Hupp, *Chem. Soc. Rev.*, 2009, **38**, 1450–1459.

10 (a) M. J. H. Ojea, C. Wilson, S. J. Coles, F. Tunac and Mark Murrie, *Dalton Trans.*, 2015, **44**, 19275–19281; (b) X. -Y. Dong, X. –Y. Li, L. –Z. Liu, H. Zhang, Y. -J. Ding and W.-K. Dong, *RSC Adv.*, 2017, **7**, 48394–48403; (c) X. -Q. Zhao, D. -X. Bao, J. Wang, S. Xiang and Y. –C. Li, *Inorganica Chimica Acta*., 2017, **466**, 110–116

11 (a) R. C. Cammarota and C. C. Lu, *J. Am. Chem. Soc.*, 2015, **137**, 12486−12489; (b) S. Ghosh, S. Biswas, A. Bauzá, M. B. -Oliver, A. Frontera, and A. Ghosh, *Inorg. Chem.*, 2013, **52**, 7508−7523.

12 G. Kumar and R. Gupta, *Chem. Soc. Rev.*, 2013, **42**, 9403–9453.

13 S. Srivastava and R. Gupta, *CrystEngComm.*, 2016, **18**, 9185-9208.

14 (a) J. B. Burnett, P. M. Barron and W. Choe, *CrystEngComm.*, 2012, **14**, 3839–3846; (b) T. Grancha, J. F.Soria, M. Castellano, M. Julve, J. Pasan, D. Armentanoc and E. Pardo, *Chem. Commun.*, 2014, **50**, 7569–7585.

15 (a) M. C. Das, S. Xiang, Z. Zhang and B. Chen, *Angew. Chem. Int. Ed.*, 2011, **50**, 10510 – 10520; (b) R. Kitaura, G. Onoyama, H. Sakamoto, R. Matsuda, S. Noro and S. Kitagawa, *Angew. Chem.*, *2004*, **116**, 2738–2741; (c) R. Kitaura, G. Onoyama, H. Sakamoto, S. Noro, R, Matsuda and S. Kitagawa, *Angew. Chem. Int. Ed.*, 2004, **43**, 2684–2687; (d) H. Sakamoto, R. Matsuda, S. Bureekaew, D. Tanaka and S. Kitagawa, *Chem. Eur. J.*, 2009, **15**, 4985–4989; (e) B. Chen, F. R. Fronczek, A.W. Maverick, *Inorg. Chem*. 2004, **43**, 8209–8211.

16 (a) M. Wang, V. Vajpayee, S. Shanmugaraju, Y.-R. Zheng, Z. Zhao, H. Kim, P. S. Mukherjee, K.-W. Chi and P. J. Stang *Inorg. Chem.*, 2011, **50**, 1506–1512; (b) S.-I. Noro, H. Miyasaka, S. Kitagawa, T. Wada, T. Okubo, M. Yamashita and T. Mitani, *Inorg. Chem.*, 2005, **44**, 133–146.

17 (a) H. Hara, A. Kobayashi, S. –I. Noro, H.-C. Changa and M. Kato, *Dalton Trans.*, 2011, **40**, 8012–8018; (b) A. Kobayashi, T. Ohba, E. Saitoh, Y. Suzuki, S.-I. Noro, H.-C. Chang and Masako Kato, *Inorg. Chem*. 2014, **53**, 2910−2921; (c) A. Kobayashi, H. Hara, T. Yonemura, H.-Chol Chang and Masako Kato, *Dalton Trans.*, 2012, **41**, 1878–1888.

18 (a) S. R. Halper, L. Do, J. R. Stork and S. M. Cohen, *J. Am. Chem. Soc.*, 2006, **128**, 15255-15268; (b) D. L. Murphy, M. R. Malachowski, C. F. Campanac and S. M. Cohen, *Chem. Commun.*, 2005, 5506–5508; (c) S. J. Garibay, J. R. Stork, Z. Wang, S. M. Cohen and S. G. Telfer. *Chem. Commun.*, 2007, 4881–4883.

19 (a) A. D. Burrows, M. F. Mahon and C. T. F. Wong, *CrystEngComm.*, 2008, **10**, 487–489; (b) A. D. Burrows, M. F. Mahon, C. L. Renouf, C. Richardson, A. J. Warrena and J. E. Warren, *Dalton Trans.*, 2012, **41**, 4153–4163.

20 (a) H. Sepehrpour, M. L. Saha, and P. J. Stang, *J. Am. Chem. Soc.*, 2017, **139**, 2553−2556; (b) M. C. Das, Q. Guo, Y. He, J. Kim, C. -G. Zhao, K. Hong, *J. Am. Chem. Soc.*, 2012, **134**, 8703−8710.

21 (a) A. Mishra, A. Ali, S. Upreti and R. Gupta, *Inorg. Chem.*, 2008, **47**, 154–161; (b) A. Mishra, A. Ali, S. Upreti, M. S. Whittingham and R. Gupta, *Inorg. Chem.*, 2009, **48**, 5234–5243; (c) A. P. Singh and R. Gupta, *Eur. J. Inorg. Chem.*, 2010, 4546–4554; (d) G. Kumar, A. P. Singh and R. Gupta, *Eur. J. Inorg. Chem.*, 2010, 5103–5112; (e) S. Srivastava, A. Ali, A. Tyagi and R. Gupta, *Eur. J. Inorg. Chem.*, 2014, 2113–2123.

22 (a) A. P. Singh, A. Ali and R. Gupta, *Dalton Trans.*, 2010, **39**, 8135–8138; (b) A. P. Singh, G. Kumar and R. Gupta, *Dalton Trans.*, 2011, **40**, 12454–12461; (c) G. Kumar and R. Gupta, *Inorg. Chem.*, 2012, **51**, 5497–5499; (d) G. Kumar and R. Gupta, *Inorg. Chem.*, 2013, **52**, 10773–10787.

23 (a) A. Ali, G. Hundal and R. Gupta, *Cryst. Growth Des.*, 2012, **12**, 1308–1319; b) G. Kumar, H. Aggarwal, R. Gupta, *Cryst. Growth Des.*, 2013, **13**, 74–90; (c) G. Kumar, G. Kumar and R. Gupta, *Inorg. Chem.*, 2015, **54**, 2603−2615.

24 (a) G. Kumar, G. Kumar and R. Gupta, *RSC Adv.*, 2016, **6**, 21352–21361; (b) S. Srivastava, V. Kumar and R. Gupta, *Cryst. Growth Des.*, 2016, **16**, 2874–2886.

25 (a) G. Kumar, F. Hussain and R. Gupta, *Dalton Trans.*, 2017, **46**, 15023–15031; (b) D. Bansal, S. Pandey, G. Hundal and R. Gupta, *New J. Chem.*, 2015, **39**, 9772–9781; (c) D. Bansal, Geeta Hundal and R. Gupta, *Eur. J. Inorg. Chem*. 2015, 1022–1032 (d) S. Srivastava, H. Aggarwal, and R. Gupta, *Cryst. Growth Des.*, 2015, **15**, 4110−4122.

26 D. Bansal, G. Kumar, G. Hundal and R. Gupta, Dalton Trans., 2014, **43**, 14865–14875; (b) D. Bansal and R. Gupta, *Dalton Trans.*, 2016, **45**, 502–507.

27 W. J. Geary, *Coord. Chem. Rev.*, 1971, **7**, 81–122.

28 L. Yang, D. R. Powell and R. P. Houser, *Dalton Trans.*, 2007, 4617–955–964.

29 M. K. Zart, T. N. Sorell, D. Powell and A. S. Borovik, *Dalton Trans.*, 2003, 1986–1992.

30 A. W. Addison, T. N. Rao, J. Reedijk, J. V. Rijn and G. C. Vershoor, *Dalton Trans.*, 1984, 1349–1356.

31 H. Yamamoto, *Lewis acids in organic synthesis*, Wiley-VCH Verlag GmbH, 2008.

32 A. Corma and H. Garcia, *Chem. Rev.* 2003, **103**, 4307-4365.

33 (a) F. Freeman, *Chem. Rev.*, 1980, **80**, 329–350; (b) L. F. Tietze, *Chem. Rev.*, 1996, **96**, 115–136.

34 (a) A. Lee, A. Michrowska, S. Sulzer-Mosse and B. List, *Angew. Chem. Int. Ed.*, 2011, **50**, 1707; (b) A. C. Brooks, L. France, C. Gayot, J. Li, H. Pui, R. Sault, A. Stafford, J. D. Wallis and M. Stockenhuber, *J. Catal.*, 2012, **285**, 10–18; (c) Y. Peng, J. Y. Wang, J. Long and G. H. Liu, *Catal. Commun.*, 2011, **15**, 10–14.

35 (a) K. K. Bania, G. V. Karunakar, K. Goutham, and R. C. Deka, *Inorg. Chem.*, 2013, **52**, 8017−8029; (b) V. J. Mayani, S. H. R. Abdi, R. I. Kureshy, N.-U. H. Khan, A. Das and H. C. Bajaj, *J. Org. Chem.*, 2010, **75**, 6191–6195; (c) T. Nitabaru, A. Nojiri, M. Kobayashi, N. Kumagai and M.

View Article Online
DOI: 10.1039/C8NJ00734A

Shibasaki, *J. Am. Chem. Soc*., 2009, **131**, 13860–13869; (d) A. Karmakar, M. F. C. G. D. Silva and A. J. L. Pombeiro, *Dalton Trans*., 2014, **43**, 7795–7810; (e) H. Li, B. Wang, and L. Deng, *J. Am. Chem. Soc*., 2006, **128**, 732–733.

36 T. Marino, N. Russo and M. Toscano. *J. Am. Chem. Soc*., 2005, **127**, 4242-4253.

37 (a) R. Ballini, G. Bosica and M. Parrini, *Tetrahedron Lett*., 1998, **39**, 7963–7964; (b) L. Bernardi, B. F. Bonini, E. Capito, G. Dessole, M. C. Franchini, M. Fochi, and A. Ricci, *J. Org. Chem*., 2004, **69**, 8168–8171.

38 (a) T. Arai, M. Watanabe and A. Yanagisawa, *Org. Lett*., 2007, **9**, 3595–3597; (b) H. Naili, F. Hajlaoui, T. Mhiri, T. C. O. Mac Leod, M. N. Kopylovich, K. T. Mahmudov and A. J. L. Pombeiro, *Dalton Trans*., 2013, **42**, 399–406.

39 K. Nakamoto, *Infrared and Raman Spectra of Inorganic and Coordination Compounds*, John Wiley & Sons, 1986.

40 D. D. Perrin, W. L. F. Armarego and D. R. Perrin, *Purification and Laboratory Chemicals*, Pergamon Press, Oxford, 1980.

41 *CrysAlisPro,ver.1.171.33.49b*, Oxford Diffraction Ltd, 2009.

42 *SMART*: *Bruker Molecular Analysis Research Tool, version 5.618*, Bruker Analytical X- ray System 2000.

43 *SAINT–NT, Version 6.04*, Bruker Analytical X-ray System, 2001.

44 *SHELXTL–NT, Version 6.10*, Bruker Analytical X-ray System, 2000.

45 A. Altomare, G. Cascarano, C. Giacovazzo, A. Guagliardi, *J. Appl. Crystallogr*. 1993, **26**, 343.

46 L. J. Farrugia, WinGX *version 1.64, An integrated system of Windows Programs for the Solution, Refinement and Analysis of Single-Crystal X-ray Diffraction Data*, Department of Chemistry, University of Glasgow, 2003.

47 A. L. Spek, PLATON, *A Multipurpose Crystallographic Tool*, version 21116, Utrecht University, The Netherlands.

View Article Online
DOI: 10.1039/C8NJ00734A

A metalloligand appended with benzimidazole rings: Tetranuclear [$CoZn_3$] and [$CoCd_3$] complexes and their catalytic applications

Saurabh Pandey, Deepak Bansal and Rajeev Gupta
Department of Chemistry, University of Delhi, Delhi – 110 007 (India)

Graphical Abstract

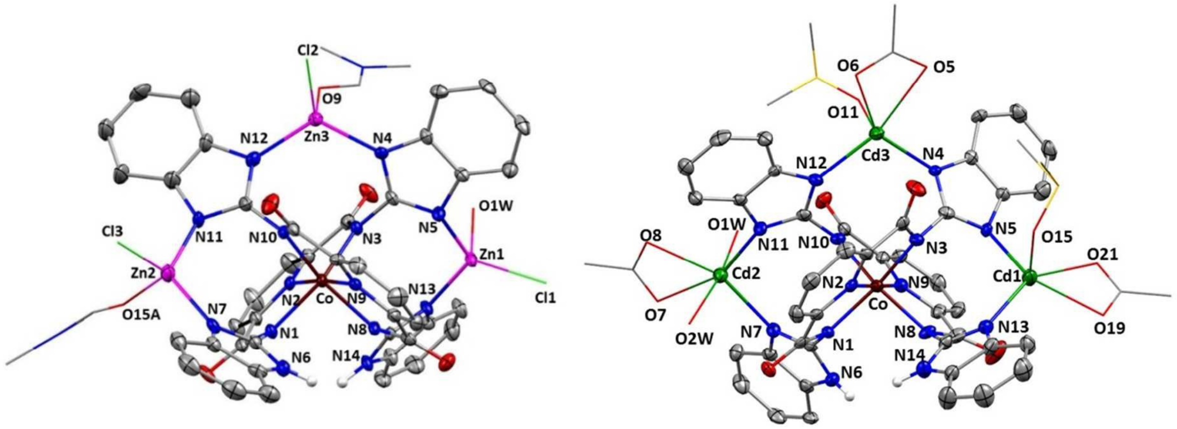

A novel Co^{3+}-based metalloligand, offering appended benzimidazole rings, has been utilized for the synthesis of catalytically active tetranuclear [$CoZn_3$] and [$CoCd_3$] heterometallic coordination complexes.